Title
Membrane and nuclear estrogen receptor a collaborate to suppress adipogenesis but not triglyceride content

Journal
The FASEB Journal, 30(1)

ISSN
0892-6638

Authors
Pedram, Ali
Razandi, Mahnaz
Blumberg, Bruce
et al.

Publication Date
2016

DOI
10.1096/fj.15-274878

Membrane and nuclear estrogen receptor α collaborate to suppress adipogenesis but not triglyceride content

Ali Pedram,* Mahnaz Razandi,* Bruce Blumberg,† and Ellis Robert Levin*,‡,§,1

*Division of Endocrinology, Veterans Affairs Medical Center, Long Beach, California, USA; †Department of Developmental and Cell Biology, ‡Department of Medicine, and §Department of Biochemistry, University of California, Irvine, Irvine, California, USA

ABSTRACT **Estrogen and estrogen receptor (ER)-α suppress visceral fat development through actions in several organs *via* unclear mechanisms that we sought to identify. Using mice that express only nuclear ER-α [nuclear-only ER-α (NOER) mice] or plasma membrane ER-α [membrane-only ER-α (MOER) mice], we found that 10-wk-old mice that lacked either receptor pool showed extensive abdominal visceral fat deposition and weight gain compared with wild-type (WT) mice. Differentiation of cultured bone marrow stem cells (BMSCs) into the adipocyte lineage was suppressed by 17-β-estradiol (E2) in WT female mice but not in NOER or MOER mice. This finding correlated with E2 inhibition of prominent differentiation genes in WT BMSCs. In contrast, triglyceride content in differentiated BMSCs or 3T3-L1 cells was suppressed as a result of membrane ER-α signaling through several kinases to inhibit carbohydrate response element–binding protein-α and -β. We concluded that extranuclear and nuclear ER-α collaborate to suppress adipocyte development, but inhibition of lipid synthesis in mature cells does not involve nuclear ER-α.—Pedram, A., Razandi, M., Blumberg, B., Levin, E. R. Membrane and nuclear estrogen receptor α collaborate to suppress adipogenesis but not triglyceride content. *FASEB J.* 30, 230–240 (2016). www.fasebj.org**

Key Words: BMSCs · preadipocytes · adipocyte hypertrophy · kinase activation · ChREBP

Estrogen promotes the reproductive fitness and overall health of premenopausal women. After menopause, many metabolic diseases in women increase in frequency, including osteoporosis, glucose intolerance, frank diabetes mellitus, and obesity (1). It is recognized that an important contributor to these diseases is the increased visceral fat that women gain shortly after menopause (2, 3). Human and rodent studies have shown that estrogen acting through estrogen receptor (ER)-α suppresses visceral fat development and resulting obesity (4, 5) and suppresses food consumption through actions at discrete hypothalamic nuclei (6). Thus, after menopause, the decrease in production of this sex steroid in the ovaries contributes to the increase in metabolic diseases that is often found in aging women.

At the level of adipocyte development, E2 and genistein act through undetermined ER isoforms to suppress human bone marrow progenitor commitment to the adipocyte lineage that underlies visceral fat development (7). Recent work on adipose niche progenitors suggests that direct ER-α action promotes subcutaneous fat development that is considered metabolically advantageous (8). TGF-β has been implicated in the effects of E2 on both bone marrow and adipocyte niche sources of stem/progenitor cells (7, 8), but additional mechanisms are likely to be important and are poorly understood. Furthermore, the functions of various ER subcellular pools that may regulate adipose progenitor differentiation are unknown. Although total ER-α knockout mice show abundant visceral fat (5), these results do not implicate any specific cellular pool of ER-α, because extranuclear and nuclear ER-α are the same protein resulting from the same mRNA (9) and are absent in the ER gene-deletion mouse (5, 10). In addition, most reports indicate that the ER-β isoform is not a major contributor to adipocyte suppression when ER-α is present (11, 12).

To understand how estrogen and ER-α suppress fat development, we investigated wild-type (WT) female mice and compared them to females from 2 transgenic mice that lack either membrane ER-α (nuclear-only ER-α; NOER) (13) or nuclear ER-α (membrane-only ER-α; MOER) (10, 14). Investigating the cells from these mice allowed us to determine which ER isoform and cellular pools contribute to the regulation of early progenitor commitment to the adipocyte lineage. In addition, we determined the effects of estrogen on preadipocyte maturation, and function of the mature adipocyte.

MATERIALS AND METHODS

Mice

The Animal Studies and the Research and Development Committees at the Department of Veterans Affairs Long Beach

Abbreviations: ACC, acetyl-CoA carboxylase; AMPK, adenosine monophosphate-activated protein kinase; aP2, fatty acid–binding protein 4; BMSC, bone marrow–derived stem cell; BrdU, 5-bromo-2′-deoxyuridine; CC, compound C; C/EBP-β, CCAAT/enhancer binding protein β; DPN, dipropyl nitrile; EDC, estrogen dendrimeric compound; ChoRE, carbohydrate

(*continued on next page*)

[1] Correspondence: Medical Service (111-I), Long Beach Veterans Affairs Medical Center/University of California, Irvine, 5901 E. 7th St., Long Beach, CA 90822, USA. E-mail: ellis.levin@va.gov

doi: 10.1096/fj.15-274878

This article includes supplemental data. Please visit *http://www.fasebj.org* to obtain this information.

0892-6638/16/0030-0230 © FASEB

Healthcare Facility approved all experiments that conform to relevant regulatory standards. Transgenic MOER and NOER mice were created as has been described (10, 13). MOER mice bear a ligand-binding domain (E domain) that is exclusively targeted to the plasma membrane of all organs and cells created on the background of total ER-α depletion. The cells show rapid signal transduction in a variety of organs *in vivo* and from isolated cells *in vitro*, identical to WT mouse organs and cells. The point mutant (C451A) knockin NOER mice show selective deletion of the plasma membrane pool that results from loss of ER palmitoylation, which is necessary for trafficking of the steroid receptor to the plasma membrane. As a result, signal transduction in response to estrogen is lost (13). All mice were fed low-fat mouse chow (8604; Teklad, Madison, WI, USA) and ~10- to 12-wk-old ovary-intact females were used for the experiments. For the abdominal visceral fat studies, the anesthetized mice were weighed, the abdomen opened, and the fat dissected from the viscera and weighed. For abdominal visceral fat determination, mean ± SEM weights for each group of 5 or more mice were calculated. The mice were euthanized, and a portion of adipose tissue was fixed in paraformaldehyde preservative to create histologic slides.

The cell surface area of adipose cells was determined from tissue that had been fixed, embedded in paraffin, and cut into 5 μm sections for mounting on slides stained with hematoxylin and eosin. The histology sections were viewed at ×10 magnification, and the images were obtained with a Spot digital camera (Diagnostic Instruments, Sterling Heights, MI, USA). The images were converted into a binary format with PhotoShop (Adobe Systems, San Jose, CA, USA) and the Image Processing Tool (Image J; National Institutes of Health, Bethesda, MD, USA). The total number and cross-sectional areas of adipocytes were calculated. The cross-sectional areas are expressed in square millimeters. Results were directly loaded into a spreadsheet (Excel; Microsoft Inc., Redmond, WA, USA). Because each millimeter of the digital image was equivalent to ~50 μm, the calculated areas were multiplied by a conversion factor of 2500 (50^2) to determine the cross-sectional area of the adipocytes in square micrometers. Values less than 100 μm^2 were assumed to represent artifacts from the image-conversion process and were excluded from analysis. Image J software was used for analysis.

Differentiation and proliferation

BMSCs were isolated from mouse tibia and fibula under in mice anesthesia, cultured as we described (15), and identified by Sca1, CD105, and CD90 protein expression, in the absence of CD19 and CD31. 3T3-L1 cells and BMSCs were grown in DMEM with 10% calf serum and no phenol red. To induce differentiation, we switched confluent cells to medium containing dialyzed 10% fetal bovine serum, 10 μg/ml insulin (Sigma-Aldrich, St. Louis, MO, USA), 1 μM dexamethasone (Sigma-Aldrich), and 0.5 mM 3-isobutyl-1-methylxanthine (IBMX; Sigma-Aldrich) for 2 d, followed by 6 d of the same differentiation medium but with either 10 μg/ml insulin or 1 μM rosiglitazone added. Control medium contained no insulin or rosiglitazone for the last 6 d. In some conditions, E2 10 nM was added for the last 6 d. Maturation of all cells was confirmed by Oil Red O staining (Sigma-Aldrich) and lipid vesicle formation.

Oil Red O staining was performed with modifications, to avoid dye precipitation during incubation with cells. For dye preparation, 0.35 g Oil Red O was dissolved in 100 ml isopropanol and left overnight at room temperature. After that, the solution was filtered from the formed precipitate. Thirty milliliters of water was added to 60 ml of the solution (0.1% working solution) and left overnight at 4°C. The working solution was filtered twice and added to the cells. Adherent cells were rinsed with PBS and fixed in 4% paraformaldehyde for 1 h, followed by rinsing with PBS once and with water twice. After the rinsing, staining with 0.1% Oil Red O was performed for 1–2 h. The plates were rinsed 3 times with water, and images of the cells on plates were taken in water. For quantification, the dye was extracted with isopropanol, and absorbance was determined at 492 nm.

The cell proliferation assay is a nonisotopic immunoassay that quantifies 5-bromo-2′-deoxyuridine (BrdU) incorporation into newly synthesized DNA of actively proliferating cells. 3T3L1 or BMSCs were seeded into a 24-well cell culture plate at a cell density of 1×10^5 cells/ml. The cells were allowed to attach and were synchronized in 0.1% serum for 24 h and treated with insulin or rosiglitazone in DMEM in the presence or absence of E2, propyl-pyrazole-triol (PPT), or dipropyl nitrile (DPN) for 48 h. The cells were then incubated with BrdU for 24 h, and the assay was performed according to the manufacturer's instructions (Abcam, Cambridge, MA, USA). The absorbance was measured with a spectrophotometer at a dual wavelengths of 450/540 nm. The results were calculated as the percentage of cell proliferation *vs.* control.

Reagents

Estrogen dendrimeric compound (EDC) was synthesized at the University of Indiana (Indianapolis, IN, USA) by previously delineated techniques (16, 17) and validated in our laboratory. Antibodies to ER-α were from Santa Cruz Biotechnology (C terminus; MC-20) (Santa Cruz, CA, USA), as were antibodies to CD90, CD19, and CD31. Sca1and CD105 antibodies were from Abcam. ER-β antibody was directed against the protein C terminus (51-7700; Life Technologies-Invitrogen Corp., Carlsbad, CA, USA). 5′-Nucleotidase (5NT), transportin, nuclear transport factor 2 (NFT2), and cytochrome *c* antibodies were from Santa Cruz Biotechnology. Phospho (Thr172) and total adenosine monophosphate–activated protein kinase (AMPK) antibodies were from Cell Signaling Technology, Inc. (Danvers, MA, USA), and phosphorylated (Thr197) and total PKA antibodies were from Santa Cruz Biotechnology. The carbohydrate response element–binding protein (ChREBP)-α antibody was from Novus Biologicals (NB400-136; Littleton, CO, USA). PPT (an ER-α agonist) and DPN (an ER-β agonist) were from Tocris Bioscience (Bristol, United Kingdom).

Triglyceride measurements

Triglyceride was extracted from cells in 200 μl of chloroform/isopropanol/NP-40 (7:11:0.1) in a microhomogenizer. Cell extracts were centrifuged for 5–10 min at 15,000 *g*, and the liquid organic phase was transferred to a new tube and air dried at 50°C to remove chloroform. The samples were put in a vacuum for 30 min to remove trace solvent. Dried lipids were dissolved in Triton X-100 in 200 μl of specific lipid assay buffer. Quantification was performed per the manufacturer's instructions (Abcam), as we described (14). For experiments, 3T3-L1 cells or BMSCs from the 3 mouse types were differentiated in medium containing rosiglitazone or

(*continued from previous page*)

response element; ChREBP, carbohydrate response element–binding protein; E2, 17-β-estradiol; ER, estrogen receptor; FASN, fatty acid synthase; FGF, fibroblast growth factor; IRX, Iroquois homeobox gene; MOER, membrane-only ER-α; NOER, nuclear-only ER-α; PPT, propyl-pyrazole-triol, qPCR, quantitative PCR; siRNA, small interfering RNA; TF, transcription factor; WT, wild-type

insulin, with or without E2 or EDC compound, and sometimes with kinase inhibitors.

Protein localization and expression

Immunofluorescence microscopy was performed according to a published procedure (9, 10). Cultured cells were incubated with specific primary antibody to the individual proteins, followed by culture with an FITC-conjugated second antibody (green) at 1:500 dilution (Vector Laboratories, Inc., Burlingame, CA, USA). The fluorescence microscopic images were obtained with an Eclipse TE-200 scope (Nikon, Melville, NY, USA) with ×200–400 magnification, at room temperature. A Diagnostic Instruments camera (model 3.2.0) was used in conjunction with Spot Advance software, to capture and transfer images to the computer. Western immunoblot analysis was performed with standard techniques (10, 13). Fractionation of 70% confluent cells was accomplished with a tight-fitting Dounce homogenizer until ~90% of the cells were broken, and the pellets were suspended in buffer containing 1 mM EDTA and DNAase and protease inhibitor cocktail (Sigma-Aldrich) and layered onto a discontinuous sucrose gradient (1.0–2.5 M). Cytosolic fractions were then centrifuged at 100,000 *g* for 1 h, to obtain membrane fractions, and nuclear fractions were isolated from the original centrifugation. Actin protein served as the loading control. Our fractionation purity techniques have been validated (10, 13).

For small interfering RNA (siRNA) studies, we transfected 2.5 μg each of the siRNAs in each well of cells, using OligoFectamine (Life Technologies-Invitrogen), and the cells were recovered and cultured for 48 h. We also used this protocol to express the E domain of ER-α targeted to the plasma membrane (1 μg pEmem plasmid per 10^6 cells) in NOER BMSCs. Immunoblots were performed 48 h after transfection, to validate the protein knockdown or specificity of the constructs. siRNAs were from Santa Cruz Biotechnology and Qiagen (Germantown, MD, USA), and the constructs used (5′–3′ orientation) are below.

PKA-α, sc-36240: a pool of 3 siRNA duplexes

sc-36240A: sense, CCAUGAAGAUCCUCGACAAtt, antisense, UUGUCGAGGAUCUUCAUGGtt; sc-36240B: sense, CCAUCCAGAUCUAUGAGAAtt, antisense, UUCUCAUAGAUCUGGAUGGtt; sc-36240C: sense, CGAGUAACUUUGACGACUAtt, antisense, UAGUCGUCAAAGUUACUCGtt; AMPKα1/2, (a pool of 3 siRNA duplexes), sc-45312A: sense, GAUGUCAGAUGGUGAAUUUtt, antisense, AAAUUCACCAUCUGACAUCtt; sc-45312B: sense, CCACUGCAAUACUAAUUGAtt, antisense, UCAAUUAGUAUUGCAGUGGtt; and sc-45312C: sense, CUACUGGAUUUCCGUAGUAtt, antisense, UACUACGGAAAUCCAGUAGtt.

Qiagen custom designed

ESR1 sense, r(GGU GGG AUA CGA AAA GAC C) dTdT, antisense, r(GGU CUU UUC GUA UCC CAC C)dTdT; and ESR2 sense, r(GCC CAA AUG UGU UGU GGC C)dTdT, antisense, r(GGC CAC AAC ACA UUU GGG C)dTdT.

Kinase activity assays

As a measure of kinase activation, phosphorylation of active sites in each kinase was detected by Western blot analysis of lysates of 3T3-L1 cells or BMSCs with antiphospho antibodies. PKA and AMPK activities were determined in cells incubated with 10 nM E2 for 10 min. H-89 (PKA inhibitor, 1 μM) and compound C (CC; AMPK inhibitor, 20 μM) were from Tocris.

PCR

For mRNA expression, cellular RNA was extracted (Qiagen, RNeasy kit). cDNA was synthesized by using the Improm-II reverse transcription system (Promega, Fitchburg, WI, USA). RT-PCR determined mRNA expression normalized to β-actin mRNA. mRNA studies in differentiated cells were from cells cultured under various experimental conditions at 24 h. Primers were designed with Primer3 (*http://frodo.wi.mit.edu/*; Whitehead Institute, Massachusetts Institute of Technology, Cambridge, MA, USA) and were blasted for specificity and annealed at 60°C, to amplify regions of approximately 95–120 bp. PCR amplicon sizes were confirmed by agarose gel electrophoresis. For quantitative (q)PCR, 500 ng of cDNA in a 50 μl reaction consisting of 25 μl SYBR Green, qPCR Supermix (Life Technology–Invitrogen), 1 μl of 10 μM forward/reverse primer stock and nuclease-free water was used. Thermocycling was performed with the iCycler (Bio-Rad, Plano, TX, USA) with a melting-curve temperature of 60°C. Primer pairs (F, forward; R, reverse) are: FAS: F 5′-ACG ACA GCA ACC TCA CGG CG-3′, R 5′-CTG CAG AGC CCG TGC CAG AC-3′; ACC: F 5′-CCT GGA GTG GCA GTG GTC TTC G-3′, R 5′-TCC TCC TCC CTC TGA GGC CTT G-3′; fatty acid binding protein 4 (aP2): F 5′-AGC ATC ATA ACC CTA GAT GGC G-3′, R 5′-CAT AAC ACA TTC CAC CAC CAG C-3′; CCAAT/enhancer binding protein β (C/EBP-β): F 5′-ACC GGG TTT CGG GAC TTG A-3′, R 5′-GTT GCG TAG TCC CGT GTC CA-3′; peroxisome proliferator-activated (PPAR)-γ: F 5′-TGT CGG TTT CAG AAG TGC CTT G-3′, R 5′-TTC AGC TGG TCG ATA TCA CTG GAG-3′; Iroquois homeobox gene (IRX)3: F 5′-GGC CGC CTC TGG GTC CCT AT-3, R 5′-GAG CGC CCA GCT GTG GGA AG-3′; adiponectin: F 5′- GGA GAG AAA GGA GAT GCA GG-3′, R 5′-CTT TCC TGC CAG GGG TTC-3′; leptin: F 5′- CAG GAT CAA TGA CAT TTC ACA CA-3′, R 5′- GCT GGT GAG GAC CTG TTG AT-3′; ChREBP-α: F 5′- AGT GCT TGA GCC TGG CCT AC-3′, R 5′- TTG TTC AGG CGG ATC TTG TC-3′; ChREBP-β: F 5′- AGC GGA TTC CAG GTG AGG-3′, R 5′- TTG TTC AGG CGG ATC TTG TC-3′; FGF21: F 5′- GTA ACG GGT GCC TTC CCA GA-3′, R 5′- ACC AGG AAA CAA CCG GTG G-3′; and β-actin F 5′- GGC TGT ATT CCC CTC CAT CG-3′, R 5′- CCA GGT TGG TAA TGC CAT GT-3′.

Statistical analysis

Most *in vitro* studies were performed 3 times, and for these studies, the mean and SEM of the parameters were analyzed by 2-way ANOVA plus Scheffé's test, at a level of significance of $P < 0.05$.

RESULTS

MOER and NOER mouse phenotypes indicate the requirement of several ER pools for adipocyte lineage suppression

The ER-α complete knockout mouse (5) shows a phenotype of visceral obesity, as we confirmed (10). To determine whether nuclear and membrane ER-α are necessary for the inhibition of adipogenesis, we examined visceral fat and total body weights in mice fed a low-fat diet *ad libitum*. Ten-week-old, homozygous NOER and MOER female mice each showed extensive abdominal visceral fat and significantly increased body weight compared with that of age-matched WT mice (**Fig. 1*A***), and the differences

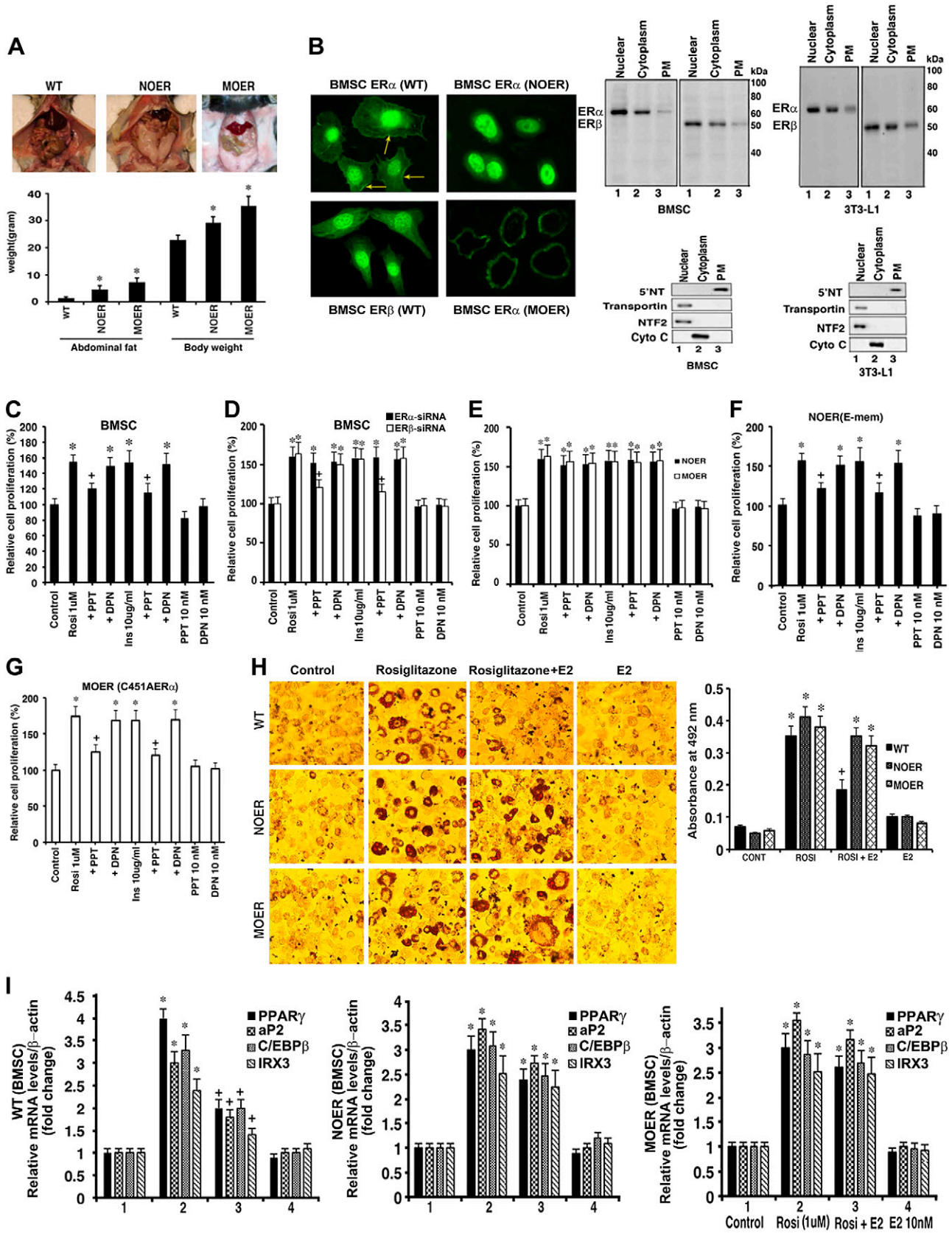

Figure 1. BMSC commitment to adipocyte lineage is suppressed by membrane and nuclear ER-α. *A*) Abdominal visceral fat and whole body weights from intact WT, MOER, and NOER female mice ($n = 5$ mice per category). Data are means ± SEM. $^*P < 0.05$ by ANOVA with Scheffé's test for WT *vs.* MOER or NOER mice. *B*) Subcellular distribution of ER-α and -β in BMSCs. Left: immunofluorescent images of ER-α and -β; right: immunoblots of fractions of WT BMSCs and 3T3-L1 cells. Bottom:

(*continued on next page*)

increased with age. These findings indicate that both membrane ER-α and nuclear ER-α play important roles in suppression of visceral fat deposition in female mice.

To further understand the effects of the receptor pools, we isolated BMSCs from WT, MOER, and NOER female mice. The cells were validated by expression of Sca1, CD105, and CD90 proteins, in the absence of CD19 and CD31, as we described (18) (Supplemental Fig. S1). We performed immunofluorescence microscopy of whole cells and immunoblot analysis of subcellular fractions, finding both ER-α and ER-β expression in the nucleus and cytoplasm, with comparatively less expression at the plasma membrane (Fig. 1*B*). Only ~5% of total endogenous ER-α is present at the membrane of multiple cell types, yet it induces rapid signal transduction in response to E2 (19). WT BMSC proliferation at 3 d of incubation was found to be significantly stimulated by the PPAR-γ agonist rosiglitazone, or by insulin. PPT, an ER-α agonist (20), significantly suppressed proliferation, but DPN, a specific ER-β agonist (21), did not (Fig. 1*C*). We then expressed specific siRNAs of each ER isoform in WT cells. Only ER-α siRNA mitigated PPT-induced inhibition of proliferation in WT BMSC (Fig. 1*D*). ER siRNAs were validated in this study (Supplemental Fig. S2) and an earlier one (22). Similar results were found for cells incubated with E2 (data not shown). These *in vitro* results are consistent with the *in vivo* fat phenotypes of total ER-α– and -β–deleted mice, where only the former are obese, with abundant visceral fat (5,10).

Having implicated ER-α, we determined which subcellular pools underlie these effects in BMSCs by comparing NOER and MOER mouse cells. PPT did not suppress stimulation of proliferation by rosiglitazone- or insulin-containing medium in cells from either mouse (Fig. 1*E*). This result suggests that membrane and nuclear ER-α pools are necessary to suppress BMSC proliferation. To support this theory, we expressed in the NOER cells the ligand-binding domain (E) of ER-α exclusively targeted to the plasma membrane. This portion of ER-α is sufficient to induce E2 to stimulate numerous signaling pathways *in vitro* and *in vivo*, comparable to the effect of endogenous membrane ER-α (10), and we used this construct to derive the MOER mouse (10, 14). Expression of the E domain at the plasma membrane restored PPT inhibition of NOER BMSC proliferation (Fig. 1*F*). We also expressed a palmitoylation-mutant ER-α (C451AER-α) in the MOER cells, a construct that precludes membrane localization but shows normal nuclear ER localization (10). C451AER-α expression supported the finding that only PPT inhibits proliferation.

We then differentiated all BMSCs by an 8 d incubation in medium, which contained rosiglitazone for the last 6 d. WT, MOER, and NOER cells responded with robust Oil Red O staining, indicating multiple lipid synthesis as a feature of mature adipocyte function, and characteristic morphology of mature cells (Fig. 1*H*). Addition of E2 strongly suppressed both aspects in rosiglitazone-induced mature WT BMSCs, but not in NOER or MOER cells. We also determined the effects of E2 on mRNAs implicated in various stages of adipocyte development and energy homeostasis (23, 24). Rosiglitazone-containing medium significantly stimulated the expression of PPAR-γ, aP2, C/EBP-β, and IRX3 mRNAs in all cells, but E2 was only inhibitory in WT BMSCs (Fig. 1*I*). Thus, both membrane and nuclear ER-αs are necessary for estrogen to suppress the genes that guide the commitment of stem cells to the adipocyte lineage.

Suppression of preadipocyte maturation and hypertrophy by ER-α

It has been reported that estrogen stimulates 3T3-L1 cells and human preadipocyte proliferation (25). Preadipocytes undergo 2 rounds of proliferation before exiting from the cell cycle to undergo differentiation. The preadipocyte 3T3-L1 cell line was therefore used for further investigation of fat cell maturation. We found that E2 and PPT, but not DPN, stimulated BrdU incorporation at 3 d, supporting the proliferative effects of ER-α (**Fig. 2*A***). In contrast, E2 significantly suppressed rosiglitazone-induced differentiation of these cells, reflected by Oil Red O staining (Fig. 2*B*). Numerous genes have been implicated in the maturation of preadipocytes or are expressed in mature adipocytes. From 2 experiments combined, rosiglitazone stimulated aP2, PPAR-γ, fibroblast growth factor (FGF)21, C/EBP-β, and adiponectin mRNAs, which were inhibited by E2 (Supplemental Table S1). The effects of E2 on cell surface area were also determined. E2 inhibited differentiation medium/rosiglitazone-induced cultured 3T3-L1 cell hypertrophy (Fig. 2*C*). In this regard, we also determined that visceral adipocytes from ovary-intact pubertal NOER and MOER mice showed increased cell surface area compared to fat cells from WT mice (Fig. 2*C*). These results indicate that the loss of either ER-α pool prevents E2-restraint of adipocyte hypertrophy.

As an additional measure of maturation, we recorded triglyceride content. The lipid was stimulated in the rosiglitazone-differentiated 3T3-L1 cells but inhibited by the sex steroid (Fig. 2D). In an important finding, EDC,

immunoblots of representative cell subfraction proteins. Representative of 2 experiments; arrows: membrane ER-α; ×10 magnification. *C*) The ER-α agonist PPT inhibited WT BMSC proliferation, shown by BrdU incorporation. $^{*}P < 0.05$ *vs.* control, $^{+}P < 0.05$ for rosiglitazone (Rosi) or insulin (Ins) *vs.* Rosi or Ins + PPT ($n = 3$ experiments). *D*) ER-α siRNA prevented PPT inhibition of cell proliferation. $^{*}P < 0.05$ *vs.* control, $^{+}P < 0.05$ for Rosi or Ins *vs.* Rosi or Ins + PPT and ER-β siRNAs ($n = 3$). *E*) PPT failed to inhibit BMSC proliferation in cells derived from NOER and MOER mice. $^{*}P < 0.05$ *vs.* control ($n = 3$). *F*) PPT inhibited proliferation in NOER BMSCs transfected to express the membrane-targeted ER-α E domain (E-mem). $^{*}P < 0.05$ *vs.* control, $^{+}P < 0.05$ for Rosi or Ins *vs.* Rosi or Ins + PPT ($n = 3$). *G*) PPT inhibited proliferation in MOER BMSCs transfected to express the palmitoylation mutant ER-α. $^{*}P < 0.05$ *vs.* control, $^{+}P < 0.05$ for Rosi or Ins *vs.* Rosi or Ins+PPT ($n = 3$). *H*) Differentiated BMSCs produced triglyceride that was inhibited by E2 only in WT cells. $^{*}P < 0.05$ *vs.* control, $^{+}P < 0.05$ for differentiation medium/Rosi *vs.* Rosi or Ins + E2 ($n = 3$). *I*) Abundances, determined by qPCR, of key mRNAs for differentiation of BMSCs was stimulated by rosiglitazone but inhibited by E2, only in WT BMSCs ($n = 3$). $^{*}P < 0.05$ *vs.* control, $^{+}P < 0.05$ *vs.* Rosi.

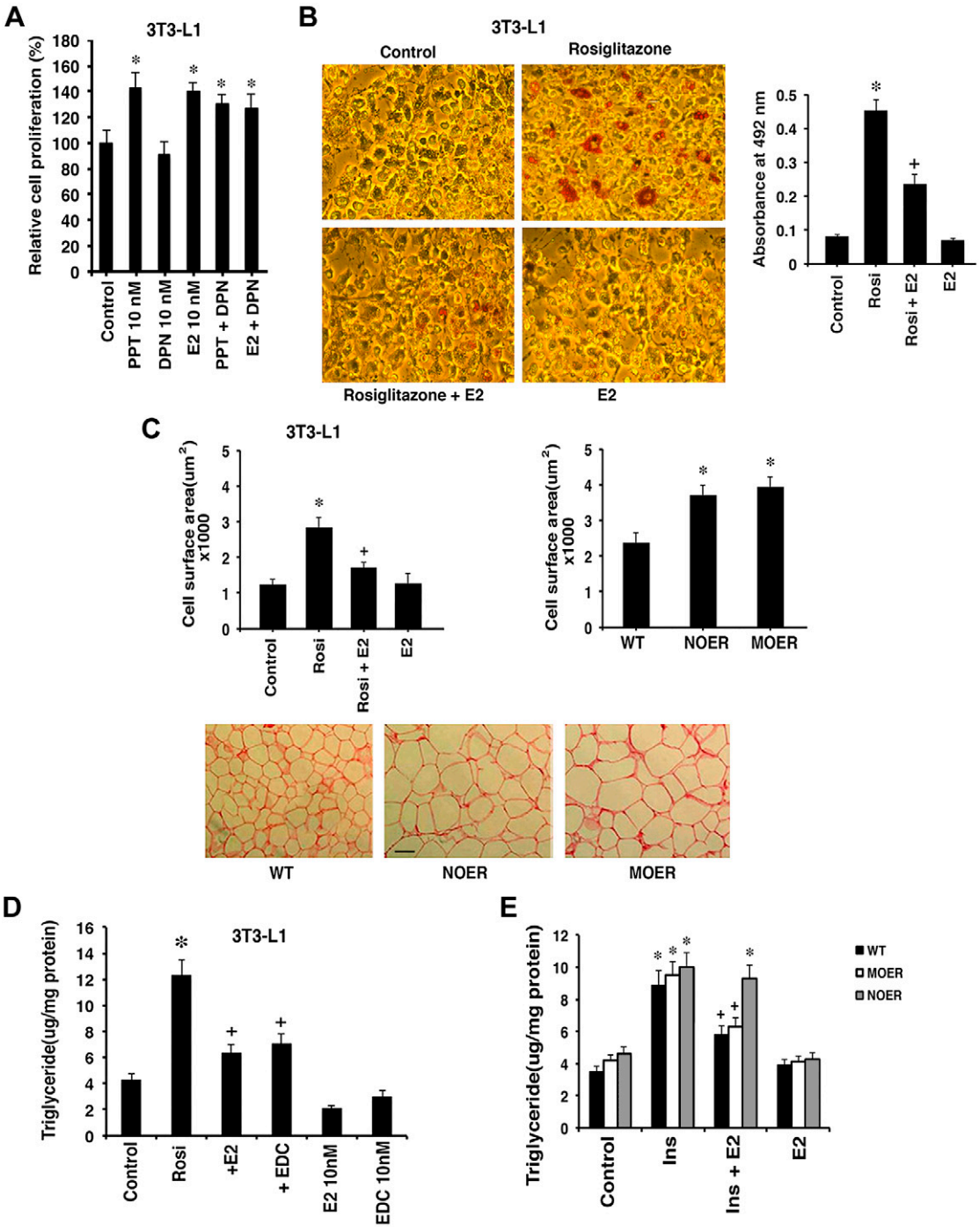

Figure 2. Membrane ER-α inhibits triglyceride content in differentiated 3T3-L1 cells. *A*) ER-α mediated E2-stimulated proliferation of 3T3-L1 preadipocytes. $^{*}P < 0.05$ *vs.* control ($n = 3$). *B*) E2 inhibited triglyceride content in differentiated 3T3-L1 cells. $^{*}P < 0.05$ *vs.* control, $^{+}P < 0.05$ *vs.* rosiglitazone ($n = 3$); ×25 magnification. *C*) E2 inhibited rosiglitazone-stimulated 3T3-L1 cell area (top left), but only in endogenous WT visceral adipocytes (top right and bottom). $^{*}P < 0.05$ for control *vs.* rosiglitazone or WT *vs.* NOER or MOER; $^{+}P < 0.05$ *vs.* rosiglitazone ($n = 3$). Scale bar, 50 μm. *D*) Membrane ER-α suppressed triglyceride content. $^{*}P < 0.05$ *vs.* control $^{+}P < 0.05$ *vs.* rosiglitazone ($n = 3$). *E*) E2 inhibited insulin-stimulated triglyceride content at 24 h in differentiated BMSCs from WT and MOER mice ($n = 3$). $^{*}P < 0.05$ *vs.* control, $^{+}P < 0.05$ *vs.* insulin.

which binds only to membrane ER, not to nuclear ER (26), inhibited triglyceride content to an extent comparable to the effect of E2 (Fig. 2*D*). This observation suggests that membrane ER-α alone is sufficient to suppress triglycerides in the mature adipocyte. To support this concept, we differentiated BMSCs for 8 d in medium containing insulin without or with E2, whereas control cells lacked insulin for the last 6 d. In the various BMSCs, differentiation resulted in enhanced triglyceride content compared to control conditions, and E2 significantly inhibited this effect in WT and MOER BMSCs, but not in NOER cells, which lack membrane ER-α (Fig. 2*E*). Because the MOER mice express

only membrane ER-α, the results indicate that membrane ER signaling alone is sufficient to repress triglycerides in differentiated adipocytes.

Membrane ER-α signaling inhibits triglyceride synthesis through suppressing ChREBP

Triglyceride synthesis in adipocytes is strongly dependent on the transcription factors (TFs), ChREBP-α and -β (27, 28). ChREBP-α stimulates expression of the ChREBP-β variant, with the latter thought to be more robust in stimulating lipid synthesis (28). We found that rosiglitazone stimulated both TF mRNAs, comparably inhibited by E2 or EDC in differentiated 3T3-L1 cells (**Fig. 3*A***).

Insulin is a well-recognized stimulant for triglyceride synthesis in many organs including fat (28). ChREBP-α/-β mRNA expression and ChREBP-α protein abundance were significantly stimulated by insulin, but the stimulation was inhibited by E2 *via* both AMPK and PKA (Fig. 3*B*). The E2 action was determined with soluble kinase inhibitors (CC for AMPK and H-89 for PKA) and siRNAs for each kinase, indicating an important role for membrane ER-α (10) (Fig. 3*B*). siRNA validation is shown in Supplemental Fig. S3. We have reported that membrane ER activation of AMPK results from PKA activation in liver cells (14), shown in adipocytes in this study, given that the PKA antagonist inhibited both kinase activities, whereas CC had no effect on PKA (Supplemental Fig. S2).

Further supporting the exclusive role of membrane ER-α, differentiated BMSCs from MOER, but not NOER, mice responded to E2 with kinase activation (Fig. 3*C*), consistent with the lack of membrane ER-α in the latter cells. Linking the signaling to function in differentiated 3T3-L1 cells, E2 suppression of insulin-stimulated triglyceride content was prevented by coexposure of the cells to either AMPK or PKA inhibitors (Fig. 3*D*).

Downstream genes that are regulated by ChREBP and are important for lipid synthesis include acetyl-CoA carboxylase (ACC) and fatty acid synthase (FASN) (28). In differentiated WT BMSCs, ACC and FAS mRNAs and proteins were stimulated by insulin, but this effect was prevented by E2 in an AMPK- and PKA-dependent fashion (Fig. 3*E*). We noted with interest that E2 inhibited only the stimulated ACC and FASN mRNAs in differentiated WT and MOER mouse stem cells, but not in NOER BMSCs (Fig. 3*F*). Thus, inhibition of key lipid synthesis genes in mature adipocytes exclusively results from membrane ER-α signaling, not requiring nuclear ER-α.

Signaling from membrane ER-α suppresses ChREBP-α cytoplasmic–nuclear translocation

How else might membrane ER-α signaling regulate the expression of ChREBP-dependent target genes in the mature adipocyte? We postulated that E2 signaling prevents the translocation of ChREBP-α from cytoplasm to the nucleus of adipocytes. Nuclear localization of the TF is necessary for ChREBP-regulated triglyceride synthesis, occurring when the nuclear pool of this TF binds to DNA carbohydrate-response elements (ChoRE) regulating target gene transcription (27). In liver, ChREBP-α binds to ChoRE in target genes after undergoing dephosphorylation by protein phosphatase 2A (28). We found that, in 3T3-L1 cells, both insulin and rosiglitazone caused ChREBP-α translocation from cytoplasm to nucleus, compared with control cells, which showed mainly cytoplasmic localization (**Fig. 4*A***). E2 substantially prevented this action of insulin or rosiglitazone, corresponding to inhibition of ACC and FAS expression (Fig. 3*A*). Furthermore, AMPK and PKA inhibitors prevented E2 inhibition of ChREBP nuclear trafficking (Fig. 4*B*). In summary, kinase activation by membrane ER-α causes cytoplasmic sequestration of a key transcription factor. As a result, insulin does not stimulate important lipid synthesis genes and triglycerides in adipocytes.

DISCUSSION

The regulation of adipocyte differentiation and function is an essential component of the metabolic state in mammals, including humans. Estrogen has differential effects in regulating white fat development, suppressing BMSC commitment to the adipocyte lineage (7), while stimulating the differentiation of the fat vascular niche stem cell (8). It is interesting that the fat vascular stem cell niche strongly contributes to more metabolically favorable subcutaneous fat (8), but how estrogen/ER-α accomplishes suppression of visceral white adipose tissue is not well understood, and whether discrete cellular pools of the sex steroid receptor are involved is unknown.

Regarding the former, we found that ER-α mediated the effects of the sex steroid, which is relevant to estrogen suppression of the visceral fat that accumulates in excess after menopause in women and is metabolically unfavorable. Also we report that ovary-intact female mice lacking either membrane or nuclear ER-α show significantly increased abdominal visceral fat after puberty compared with that in WT mice. At the level of BMSCs, membrane ER-α and nuclear ER-α (and not ER-β) are each needed to suppress commitment to the adipocyte lineage. This necessity is reflected by the failure of E2 to suppress key genes recognized as mediators of BMSC commitment and mature fat cell development, as observed in NOER and MOER female mice cells. In contrast, E2 inhibited aP2, PPAR-γ, FGF21, C/EBP-β, IRX3, and adiponectin mRNAs in BMSCs from WT mice and 3T3-L1 cells. As a result, E2 inhibited WT BMSC proliferation and differentiation into adipocytes. The failure of E2 to suppress BMSC proliferation in the NOER cells was rescued by expressing the E domain of ER-α, targeted exclusively to the plasma membrane, restoring signal transduction, as we have shown (13). Also, expressing the C451AER-α mutant steroid receptor that restored nuclear ER-α allowed PPT to inhibit proliferation in MOER cells. Precisely how both pools collaborate to repress transcription warrants further extensive investigation. It is likely to involve complex epigenetic and genomic mechanisms.

A key function of the fully differentiated adipocyte is to synthesize and store lipids, especially triglycerides. We

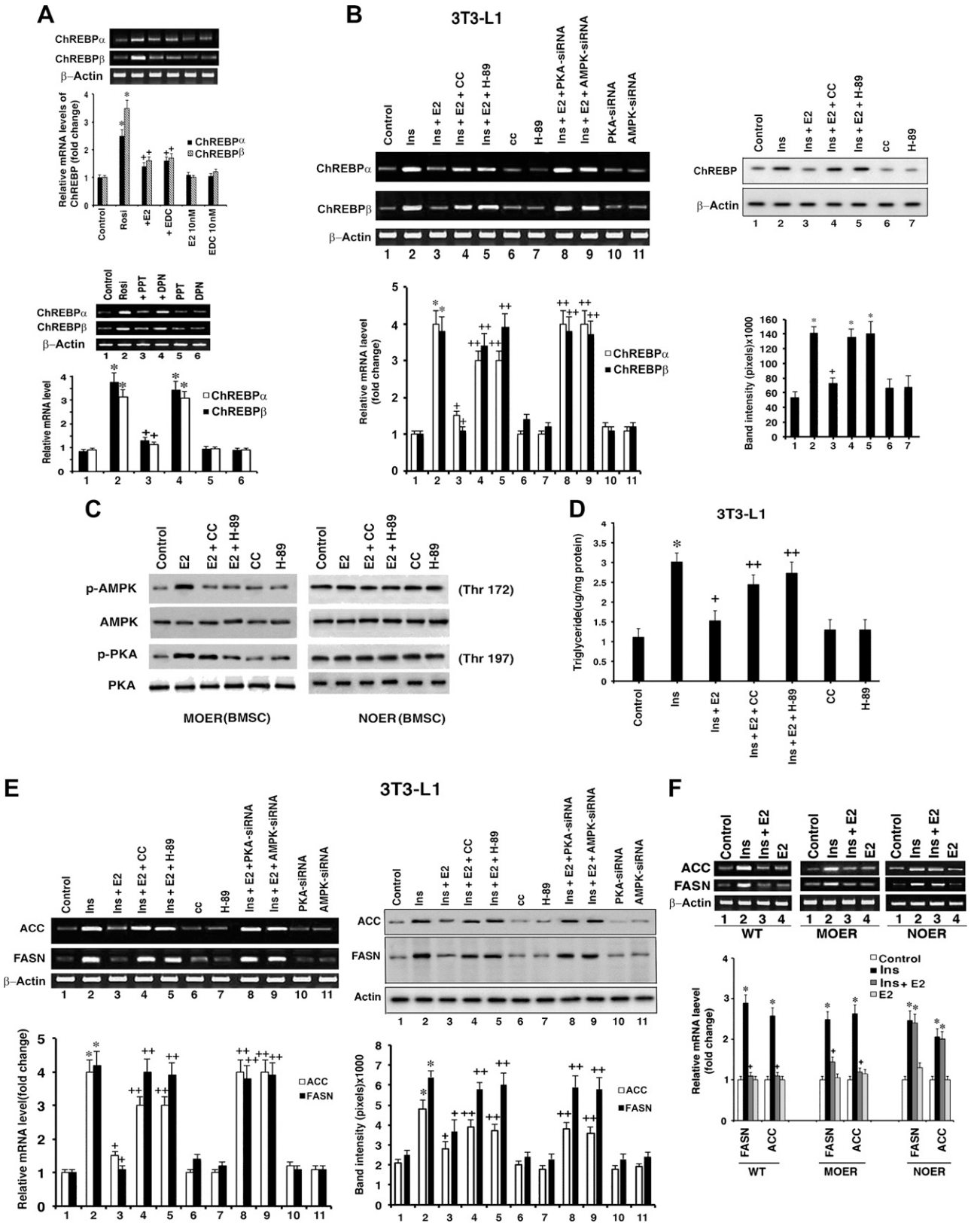

Figure 3. ChREBP is a target for membrane ER-α regulation of adipocyte function. *A*) Membrane ER-α suppressed insulin-stimulated ChREBP-α and -β mRNAs in differentiated 3T3-L1 cells, determined by RT-PCR. β-Actin was the loading control. $*P < 0.05$ *vs.* control, $^{+}P < 0.05$ *vs.* rosiglitazone ($n = 3$). *B*) E2 signaled through PKA and AMPK to inhibit insulin-stimulated ChREBP mRNAs (left) and protein (right). $*P < 0.05$ *vs.* control, $^{+}P < 0.05$ *vs.* insulin, $^{++}P < 0.05$ for insulin + E2 *vs.* insulin + E2 + CC (AMPK inhibitor), H-89 (PKA inhibitor), or specific siRNA ($n = 3$). *C*) E2 stimulates AMPK and PKA activity only in MOER BMSCs, reflected in phosphoimmunoblot analysis. Total AMPK and PKA proteins were the loading controls, and the study was

(*continued on next page*)

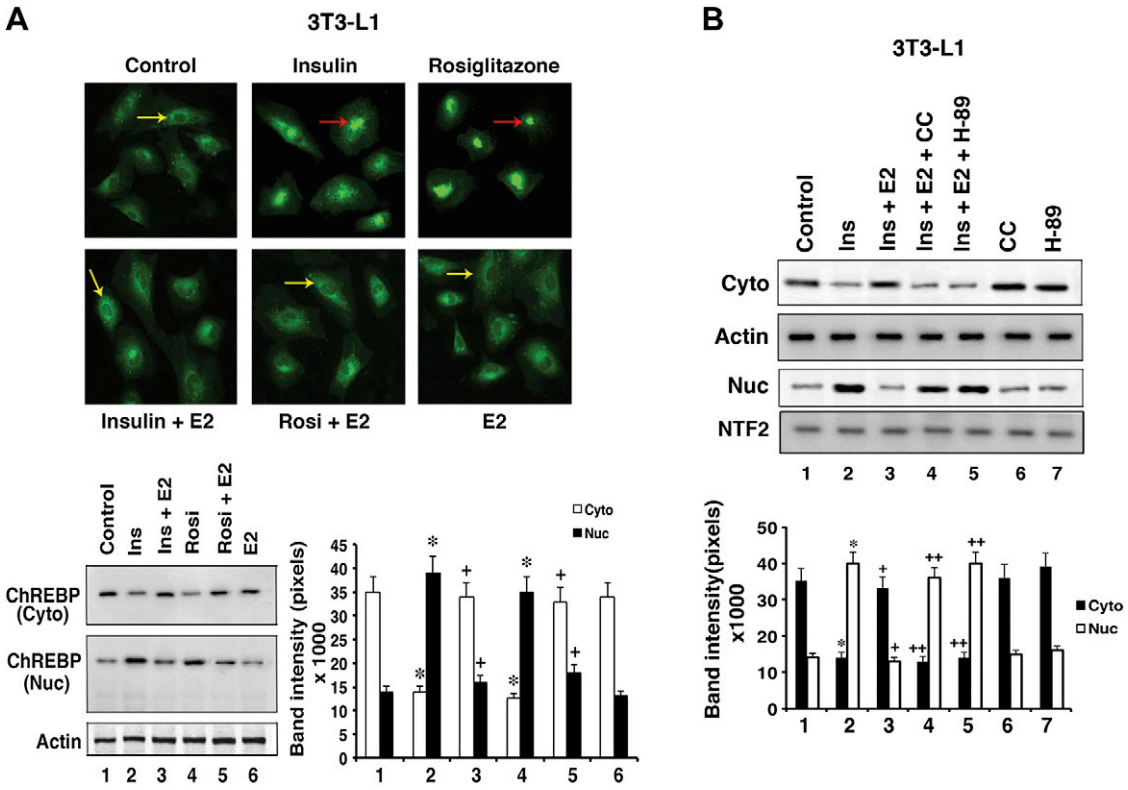

Figure 4. Trafficking of ChREBP is inhibited by membrane ER-α signaling. *A*) Insulin or rosiglitazone promotes endogenous ChREBP-α protein translocation to the nucleus of differentiated 3T3-L1 cells, but E2 blocks this process. Top: immunofluorescent images of protein localization; bottom: immunoblot subcellular localization. β-Actin in cytoplasm was the loading control. Red arrows: nuclear localization; yellow arrows: cytoplasmic localization. $*P < 0.05$ *vs.* control, $^{+}P < 0.05$ insulin or rosiglitazone *vs.* insulin or rosiglitazone + E2 ($n = 3$). *B*) E2 inhibition of ChREBP trafficking to the nucleus depended on AMPK and PKA. $*P < 0.05$ *vs.* control. $^{+}P < 0.05$ for insulin *vs.* insulin + E2, $^{++}P < 0.05$ for insulin + E2 *vs.* insulin + CC or H-89.

found in differentiated WT BMSCs and 3T3-L1 cells that E2 or EDC acting through membrane ER-α was sufficient to suppress triglyceride content (*i.e.*, did not require nuclear ER-α participation). This potentially important finding is also deduced from E2-inhibiting triglycerides in differentiated MOER but not NOER BMSCs. Tiano and Mauvais-Jarvis (29) reported that membrane ER-α signals through STAT3 to inhibit ChREBP mRNA and protein and through AMPK to reduce expression of sterol regulatory element binding protein (SREBP)-1 and fatty acid synthase expression in pancreatic islet β cells. Triglyceride suppression in mature adipocytes occurs from membrane ER-α signaling through AMPK and PKA, to inhibit expression of ChREBP-α and -β mRNAs and the cytoplasmic sequestration of ChREBP-α. ChREBP is essential for triglyceride and other lipid synthesis in adipocytes after translocation to the nucleus (27). Specifically, membrane ER-α signaling inhibits insulin and rosiglitazone stimulation of ACC and FASN mRNA (genes that are transcriptional targets for ChREBP), to stimulate lipid synthesis (28). Thus, several key genes that are essential for adipocyte function are repressed exclusively by membrane ER-α signaling. ChREBP knockdown and decreased lipogenesis in liver leads to reduced malonyl-CoA concentrations, enhancing fatty acid β-oxidation and insulin sensitivity (30, 31). Enhanced insulin sensitivity is known to result from estrogen action (32). Excessive adipocyte lipolysis from high-fat feeding or diabetes models provides a substrate for both excessive hepatic lipid synthesis and gluconeogenesis (33–35). Our findings suggest that the known effect of estrogen to oppose such altered metabolism (36, 37) could occur in part from membrane ER-α signaling, to inhibit ChREBP and triglycerides in mature adipocytes.

We have shown in earlier work that membrane ER rapidly signals to the posttranslational modification of several TFs, sequestering them in the cytoplasm of cultured heart cells, and we confirmed the findings *in vivo* (38, 39). Cytoplasmic sequestration occurs in part from

performed 2 times. *D*) AMPK and PKA mediated membrane ER-α inhibition of triglyceride. $*P < 0.05$ *vs.* control, $^{+}P < 0.05$ *vs.* insulin, $^{++}P < 0.05$ *vs.* insulin + E2 ($n = 3$). *E*) ACC and FASN mRNAs (left) and proteins (right) were stimulated by insulin but suppressed by E2 *via* PKA and AMPK. $*P < 0.05$ *vs.* control, $^{+}P < 0.05$ *vs.* insulin, $^{++}P < 0.05$ for insulin + E2 *vs.* insulin + CC, H-89, or specific siRNA ($n = 3$). *F*) E2 inhibited insulin-stimulated ACC and FASN mRNAs in differentiated WT and MOER, but not in NOER, BMSCs ($n = 3$). $*P < 0.05$ *vs.* control, $^{+}P < 0.05$ *vs.* insulin.

rapid activation of kinases or inhibition of phosphatases and results in the suppression of pathologic states in the heart. The regulation of lipid synthesis and storage in adipocytes must be closely regulated, and membrane ER-α provides some of this input though kinase activation. Although E2 is thought to act primarily as a reproduction-regulating steroid, ERs are present in almost every cell and organ in the body, often with no obvious connection to fertility. We speculate that their presence ensures the health of female mammals, including women during the reproductive years, to promote the survival of the species. In general, rapid signal transduction from membrane ERs affects the gene transcription that often occurs from collaboration with nuclear ERs (14). However, in this study, membrane ER-α–induced signaling alone inhibited the mRNAs that are necessary for lipid synthesis. Overall, both receptor pools collaboratively suppress adipogenesis, potentially contributing to a healthy metabolic state. FJ

This work was supported by a grant from the Research Service of the Department of Veteran's Affairs (to E.R.L), and Grant CA-10036 from the U.S. National Institutes of Health, Institute of Cancer Research (to E.R.L.). A.P. and M.R. performed the research, and E.R.L. and B.B. designed the research and analyzed the data. E.R.L. wrote the paper. B.B. is a named inventor on U.S. patents 5,861,274; 6,200,802; 6,815,168; and 7,250,273 related to PPAR-γ. The remaining authors declare no conflicts of interest.

REFERENCES

1. Utian, W. H. (1987) Overview on menopause. *Am. J. Obstet. Gynecol.* **156**, 1280–1283
2. Haarbo, J., Marslew, U., Gotfredsen, A., and Christiansen, C. (1991) Postmenopausal hormone replacement therapy prevents central distribution of body fat after menopause. *Metabolism* **40**, 1323–1326
3. Gambacciani, M., Ciaponi, M., Cappagli, B., Piaggesi, L., De Simone, L., Orlandi, R., and Genazzani, A. R. (1997) Body weight, body fat distribution, and hormonal replacement therapy in early postmenopausal women. *J. Clin. Endocrinol. Metab.* **82**, 414–417
4. Okura, T., Koda, M., Ando, F., Niino, N., Ohta, S., and Shimokata, H. (2003) Association of polymorphisms in the estrogen receptor alpha gene with body fat distribution. *Int. J. Obes. Relat. Metab. Disord.* **27**, 1020–1027
5. Heine, P. A., Taylor, J. A., Iwamoto, G. A., Lubahn, D. B., and Cooke, P. S. (2000) Increased adipose tissue in male and female estrogen receptor-alpha knockout mice. *Proc. Natl. Acad. Sci. USA* **97**, 12729–12734
6. Xu, Y., Nedungadi, T. P., Zhu, L., Sobhani, N., Irani, B. G., Davis, K. E., Zhang, X., Zou, F., Gent, L. M., Hahner, L. D., Khan, S. A., Elias, C. F., Elmquist, J. K., and Clegg, D. J. (2011) Distinct hypothalamic neurons mediate estrogenic effects on energy homeostasis and reproduction. *Cell Metab.* **14**, 453–465
7. Heim, M., Frank, O., Kampmann, G., Sochocky, N., Pennimpede, T., Fuchs, P., Hunziker, W., Weber, P., Martin, I., and Bendik, I. (2004) The phytoestrogen genistein enhances osteogenesis and represses adipogenic differentiation of human primary bone marrow stromal cells. *Endocrinology* **145**, 848–859
8. Lapid, K., Lim, A., Clegg, D. J., Zeve, D., and Graff, J. M. (2014) Oestrogen signalling in white adipose progenitor cells inhibits differentiation into brown adipose and smooth muscle cells. *Nat. Commun.* **5**, 5196
9. Pedram, A., Razandi, M., Kim, J. K., O'Mahony, F., Lee, E. Y., Luderer, U., and Levin, E. R. (2009) Developmental phenotype of a membrane only estrogen receptor α (MOER) mouse. *J. Biol. Chem.* **284**, 3488–3495
10. Pedram, A., Razandi, M., and Levin, E. R. (2006) Nature of functional estrogen receptors at the plasma membrane. *Mol. Endocrinol.* **20**, 1996–2009
11. Kuiper, G. G., Enmark, E., Pelto-Huikko, M., Nilsson, S., and Gustafsson, J. A. (1996) Cloning of a novel receptor expressed in rat prostate and ovary. *Proc. Natl. Acad. Sci. USA* **93**, 5925–5930
12. Seidlová-Wuttke, D., Prelle, K., Fritzemeier, K. H., and Wuttke, W. (2008) Effects of estrogen receptor alpha- and beta-selective substances in the metaphysis of the tibia and on serum parameters of bone and fat tissue metabolism of ovariectomized rats. *Bone* **43**, 849–855
13. Pedram, A., Razandi, M., Lewis, M., Hammes, S., and Levin, E. R. (2014) Membrane-localized estrogen receptor α is required for normal organ development and function. *Dev. Cell* **29**, 482–490
14. Pedram, A., Razandi, M., O'Mahony, F., Harvey, H., Harvey, B. J., and Levin, E. R. (2013) Estrogen reduces lipid content in the liver exclusively from membrane receptor signaling. *Sci. Signal.* **6**, ra36
15. Chamorro-García, R., Sahu, M., Abbey, R. J., Laude, J., Pham, N., and Blumberg, B. (2013) Transgenerational inheritance of increased fat depot size, stem cell reprogramming, and hepatic steatosis elicited by prenatal exposure to the obesogen tributyltin in mice. *Environ. Health Perspect.* **121**, 359–366
16. Trogden, B. G., Kim, S. H., Lee, S., and Katzenellenbogen, J. A. (2009) Tethered indoles as functionalizable ligands for the estrogen receptor. *Bioorg. Med. Chem. Lett.* **19**, 485–488
17. Wong, W. P., Tiano, J. P., Liu, S., Hewitt, S. C., Le May, C., Dalle, S., Katzenellenbogen, J. A., Katzenellenbogen, B. S., Korach, K. S., and Mauvais-Jarvis, F. (2010) Extranuclear estrogen receptor-alpha stimulates NeuroD1 binding to the insulin promoter and favors insulin synthesis. *Proc. Natl. Acad. Sci. USA* **107**, 13057–13062
18. Kirchner, S., Kieu, T., Chow, C., Casey, S., and Blumberg, B. (2010) Prenatal exposure to the environmental obesogen tributyltin predisposes multipotent stem cells to become adipocytes. *Mol. Endocrinol.* **24**, 526–539
19. Levin, E. R. (2014) Extranuclear estrogen receptor's roles in physiology: lessons from mouse models. *Am. J. Physiol. Endocrinol. Metab.* **307**, E133–E140
20. Harris, H. A., Katzenellenbogen, J. A., and Katzenellenbogen, B. S. (2002) Characterization of the biological roles of the estrogen receptors, ERalpha and ERbeta, in estrogen target tissues in vivo through the use of an ERalpha-selective ligand. *Endocrinology* **143**, 4172–4177
21. Meyers, M. J., Sun, J., Carlson, K. E., Marriner, G. A., Katzenellenbogen, B. S., and Katzenellenbogen, J. A. (2001) Estrogen receptor-β potency-selective ligands: structure-activity relationship studies of diarylpropionitriles and their acetylene and polar analogues. *J. Med. Chem.* **44**, 4230–4251
22. Razandi, M., Pedram, A., Jordan, V. C., Fuqua, S., and Levin, E. R. (2013) Tamoxifen regulates cell fate through mitochondrial estrogen receptor beta in breast cancer. *Oncogene* **32**, 3274–3285
23. Smemo, S., Tena, J. J., Kim, K-H., Gamazon, E. R., Sakabe, N. J., Gómez-Marín, C., Aneas, I., Credidio, F. L., Sobreira, D. R., Wasserman, N. F., Lee, J. H., Puviindran, V., Tam, D., Shen, M., Son, J. E., Vakili, N. A., Sung, H. K., Naranjo, S., Acemel, R. D., Manzanares, M., Nagy, A., Cox, N. J., Hui, C. C., Gomez-Skarmeta, J. L., and Nóbrega, M. A. (2014) Obesity-associated variants within FTO form long-range functional connections with IRX3. *Nature* **507**, 371–375
24. Rosen, E. D., and Spiegelman, B. M. (2014) What we talk about when we talk about fat. *Cell* **156**, 20–44DOI:
25. Anderson, L. A., McTernan, P. G., Barnett, A. H., and Kumar, S. (2001) The effects of androgens and estrogens on preadipocyte proliferation in human adipose tissue: influence of gender and site. *J. Clin. Endocrinol. Metab.* **86**, 5045–5051
26. Harrington, W. R., Kim, S. H., Funk, C. C., Madak-Erdogan, Z., Schiff, R., Katzenellenbogen, J. A., and Katzenellenbogen, B. S. (2006) Estrogen dendrimer conjugates that preferentially activate extranuclear, nongenomic versus genomic pathways of estrogen action. *Mol. Endocrinol.* **20**, 491–502
27. Kawaguchi, T., Takenoshita, M., Kabashima, T., and Uyeda, K. (2001) Glucose and cAMP regulate the L-type pyruvate kinase gene by phosphorylation/dephosphorylation of the carbohydrate response element binding protein. *Proc. Natl. Acad. Sci. USA* **98**, 13710–13715

28. Herman, M. A., Peroni, O. D., Villoria, J., Schön, M. R., Abumrad, N. A., Blüher, M., Klein, S., and Kahn, B. B. (2012) A novel ChREBP isoform in adipose tissue regulates systemic glucose metabolism. *Nature* **484**, 333–338
29. Tiano, J. P., and Mauvais-Jarvis, F. (2012) Molecular mechanisms of estrogen receptors' suppression of lipogenesis in pancreatic β-cells. *Endocrinology* **153**, 2997–3005
30. Dentin, R., Benhamed, F., Hainault, I., Fauveau, V., Foufelle, F., Dyck, J. R., Girard, J., and Postic, C. (2006) Liver-specific inhibition of ChREBP improves hepatic steatosis and insulin resistance in ob/ob mice. *Diabetes* **55**, 2159–2170
31. Monsénégo, J., Mansouri, A., Akkaoui, M., Lenoir, V., Esnous, C., Fauveau, V., Tavernier, V., Girard, J., and Prip-Buus, C. (2012) Enhancing liver mitochondrial fatty acid oxidation capacity in obese mice improves insulin sensitivity independently of hepatic steatosis. *J. Hepatol.* **56**, 632–639
32. Riant, E., Waget, A., Cogo, H., Arnal, J. F., Burcelin, R., and Gourdy, P. (2009) Estrogens protect against high-fat diet-induced insulin resistance and glucose intolerance in mice. *Endocrinology* **150**, 2109–2117
33. Kabashima, T., Kawaguchi, T., Wadzinski, B. E., and Uyeda, K. (2003) Xylulose 5-phosphate mediates glucose-induced lipogenesis by xylulose 5-phosphate-activated protein phosphatase in rat liver. *Proc. Natl. Acad. Sci. USA* **100**, 5107–5112
34. Shulman, G. I. (2014) Ectopic fat in insulin resistance, dyslipidemia, and cardiometabolic disease. *N. Engl. J. Med.* **371**, 1131–1141
35. Perry, R. J., Camporez, J. P., Kursawe, R., Titchenell, P. M., Zhang, D., Perry, C. J., Jurczak, M. J., Abudukadier, A., Han, M. S., Zhang, X. M., Ruan, H. B., Yang, X., Caprio, S., Kaech, S. M., Sul, H. S., Birnbaum, M. J., Davis, R. J., Cline, G. W., Petersen, K. F., and Shulman, G. I. (2015) Hepatic acetyl CoA links adipose tissue inflammation to hepatic insulin resistance and type 2 diabetes. *Cell* **160**, 745–758
36. Yonezawa, R., Wada, T., Matsumoto, N., Morita, M., Sawakawa, K., Ishii, Y., Sasahara, M., Tsuneki, H., Saito, S., and Sasaoka, T. (2012) Central versus peripheral impact of estradiol on the impaired glucose metabolism in ovariectomized mice on a high-fat diet. *Am. J. Physiol. Endocrinol. Metab.* **303**, E445–E456
37. Hong, J., Holcomb, V. B., Kushiro, K., and Núñez, N. P. (2011) Estrogen inhibits the effects of obesity and alcohol on mammary tumors and fatty liver. *Int. J. Oncol.* **39**, 1443–1453
38. Pedram, A., Razandi, M., Aitkenhead, M., and Levin, E. R. (2005) Estrogen inhibits cardiomyocyte hypertrophy in vitro: antagonism of calcineurin-related hypertrophy through induction of MCIP1. *J. Biol. Chem.* **280**, 26339–26348
39. Pedram, A., Razandi, M., O'Mahony, F., Lubahn, D., and Levin, E. R. (2010) Estrogen receptor-beta prevents cardiac fibrosis. *Mol. Endocrinol.* **24**, 2152–2165

Received for publication April 30, 2015.
Accepted for publication August 31, 2015.